

Gating the Rectifying Direction of Tunneling Current through Single-Molecule Junctions

Haoyu Wang, Fenglu Hu, Adila Adijiang, Ramya Emusani, Jieyi Zhang, Qihong Hu, Xuefeng Guo, Takhee Lee, Lichuan Chen,* and Dong Xiang*



Cite This: *J. Am. Chem. Soc.* 2024, 146, 35347–35355



Read Online

ACCESS |



Metrics & More

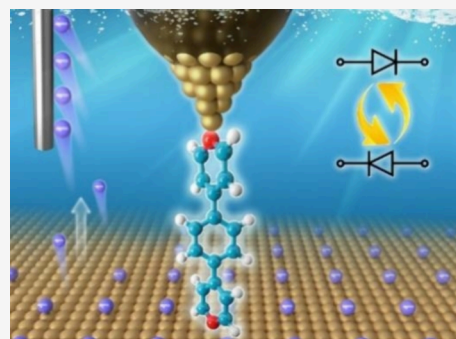


Article Recommendations



Supporting Information

ABSTRACT: In electronic functional chips, one of the most crucial components is the field-effect transistor (FET). To meet the urgent demands for further miniaturization of electronic devices, solid-state single-molecule transistors by molecular orbital gating have been extensively reported. However, under negative bias and positive bias, achieving a distinct gating effect is extremely challenging because molecular orbital gating is independent of the bias polarity. Here, we demonstrated that rectifiers can be realized in single-molecule junctions with a symmetric molecular structure and an electrode material by simply breaking the symmetry of the electrode's chemical potential via ionic adsorption. We further demonstrated that the tunneling current can be gated with opposite change tendencies under negative and positive bias by applying an ionic gating voltage, which eventually results in a reversal of the rectifying direction. Our experiments elucidate that, unlike the classical mechanism for solid molecular FET, the modulation of the electrode's chemical potential, rather than the regulation of molecular orbitals, might dominate the electron transport in the ionic liquid environment upon a gating voltage. Our study gains deeper insights into the mechanism of ionic liquid gating and opens a window for designing high-performance electrochemical-based functional devices.



INTRODUCTION

The field of single-molecule electronics has attracted a lot of attention since it not only provides a platform for observing the novel phenomena distinguished from bulk materials but also provides a potential for further miniaturization of electronic components.^{1–3} For the fabrication of single-molecule-based functional devices, controlling the tunneling current transport through the molecule is a critical step.^{3–6} A molecular junction coupled with a solid gate electrode in a three-terminal transistor configuration provides a knob to tune the electron transport characteristics effectively, which enhances the prospects for molecularly engineered electronic devices.^{7–9} Despite these great advancements, creating molecular transistors encounters challenges because it requires placing the gate electrode close enough to the molecular junction to achieve the required gate field.^{10–12} Electrochemical gating provides a promising strategy to address these challenges^{13,14} since it can provide the required gate field with liquid dielectric without rigorous requirements for the control of gate electrode position.^{13,15,16} Several groups have successfully applied the electrochemical gating technique to efficiently regulate the electron transport with either electrochemically active molecules^{12,17–20} or electrochemically inactive molecules.^{21–24}

Despite the potential of electrochemical gating, two critical issues need to be clarified: (1) Is it possible to create a bias-dependent molecular transistor, i.e., is it possible to make an

opposite gating effect on the electron transport under negative bias and positive bias? In typical single-molecule transistors, the modulation of molecular orbital by gating voltage is independent of the bias polarity, e.g., placing a more positive charge near the molecule results in a downshift of the molecular orbitals regardless of the bias polarity.^{10,21,23} (2) The underlying mechanism for the electrochemical gating, especially for the ionic liquid gating, has not been fully elucidated. It has been widely accepted that the molecular conduction orbital can be modulated by the gating voltage in a solid molecular transistor.^{7,10} However, it is not clarified if this mechanism can be fully adopted for ionic liquid gating, and it is wondered if there are new mechanisms that dominate the electron transport in the ionic gating processes.^{8,25}

Meanwhile, rectifiers, allowing electric current to flow in one direction while suppressing it in the opposite direction, are another fundamental element for current control in modern electronic devices.^{26–28} Typically, single-molecule rectification strategies involve a highly asymmetric molecule backbone (e.g.,

Received: October 1, 2024

Revised: December 5, 2024

Accepted: December 5, 2024

Published: December 13, 2024



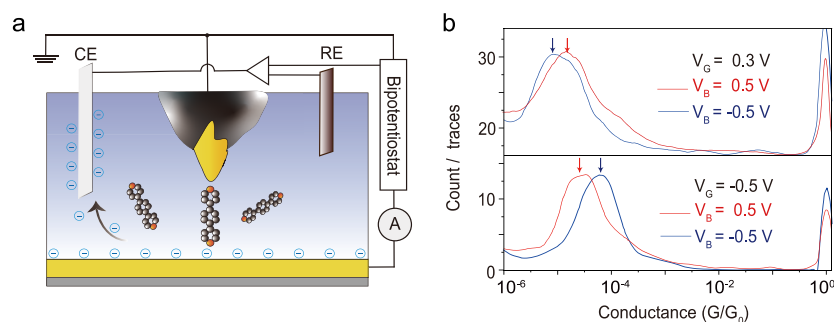


Figure 1. Conductance of ionic liquid-gated single-molecule junction. (a) Schematic of the molecular junction created by STM-BJ with a four-electrode configuration. The anions adsorbed on the substrate move toward the CE when a positive bias is applied to it. (b) Logarithmic one-dimensional conductance histogram of BPB under a bias voltage of ± 0.5 V upon a positive gating voltage (top panel) and a negative gating voltage (bottom panel). The arrows indicate the most probable conductance under different biases and gating voltages.

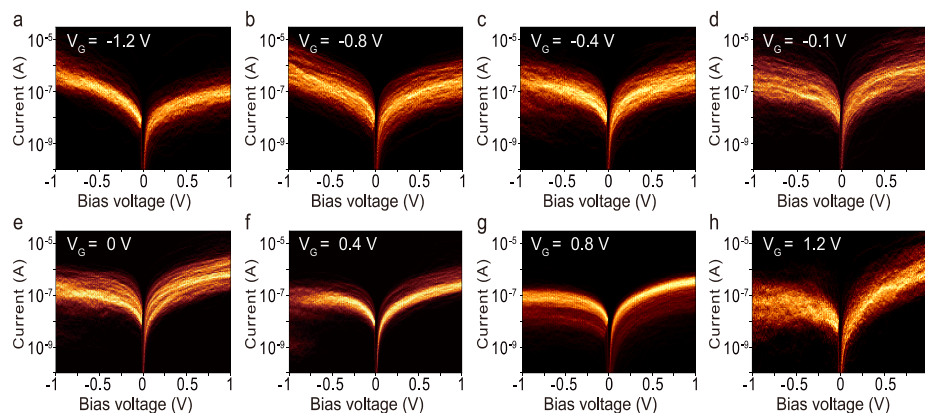


Figure 2. Two-dimensional histograms of the I - V curves. (a–h) Density maps of I - V curves of the BPB molecular junction in $[\text{BMI}]^+[\text{PF}_6]^-$ ionic liquid upon different gating voltages. The reversal of the rectifying direction of the current can be observed when the gating voltage is changed from a negative value (-1.2 V) to a positive value (1.2 V).

including two localized molecular orbitals along the molecular backbone with the D- σ -A system),^{29–37} an asymmetric molecule–electrode linker/contact,^{29,38,39} and different electrode materials at the two terminals.⁴⁰ It has been reported that the rectification ratio can be strongly modulated by electrolyte concentration,^{22,41} intermolecular *van der Waals* forces,⁴² the dipole of the molecular core,^{43,44} and solid-back/edge-on gating.^{45,46} Nevertheless, to the best of our knowledge, in situ reversal of the rectifying direction by gating voltage with the same target single-molecule has not yet been reported.

In this study, we achieve single-molecule rectification with symmetric molecular structures and electrode materials via asymmetric ion adsorption. We further demonstrate that the rectifying direction can be reversed by controlling the ionic gating voltage, showing the prototype of a single molecular bidirectional thyristor.⁴⁷ We observed that the current increases continuously with the decreasing negative gating voltage, which cannot be explained by the mechanism of the molecular orbital gating. These observations reveal that, opposite to the mechanism of a typical solid FET, modulation of the electrode's chemical potential rather than regulation of molecular orbitals by the gating voltage might dominate the electron transport in the ionic liquid environment.

Conductance of Single-Molecule Junctions. The scanning tunneling microscopy break junction (STM-BJ) with a four-electrode configuration under electrochemical conditions was utilized as the experimental platform,^{48,49} as depicted in Figure 1a. The grounded top gold tip, encapsulated

with Apiezon wax to reduce the leakage current, serves as the drain electrode (Supplementary Figure S1). The bias voltage (V_B) is applied on the bottom substrate, which serves as the source electrode. The ions adsorbed on the surface of the biased electrodes can form an electric double layer (EDL),^{44,50–52} which can be modulated by the gating voltage due to the attraction force between ions and the gate electrode (Ag/AgCl reference electrode, RE), leading to the changes in the electrode's chemical potential (work function) and thus the regulation of tunneling current.⁵² The applied gate voltage is defined as the potential difference between the coated Au tip and the RE. However, the potential of the counter electrode (CE) with the same polarity as RE is always higher than that of RE in our system. Therefore, the CE plays a more important role in modulating the EDL compared to RE. The target molecule, 1,4-bis(pyridine-4-yl) benzene (BPB) with the lowest unoccupied molecular orbital (LUMO) as the conduction channel,⁵³ was studied. Imidazolium-based ionic liquids, 1-butyl-3-methylimidazolium hexafluorophosphate ($[\text{BMI}]^+[\text{PF}_6]^-$), were used as gating dielectrics. These anions and cations with different sizes and planar geometry tend to form a densely packed layer at the electrode surface.⁵⁴ An asymmetric electrostatic environment around the junction will be generated when the bias polarity is reversed (Supplementary Figure S2).

Figure 1b shows the conductance histograms of molecular junctions under different bias and gating voltages. Each histogram is constructed from approximately 3000 individual

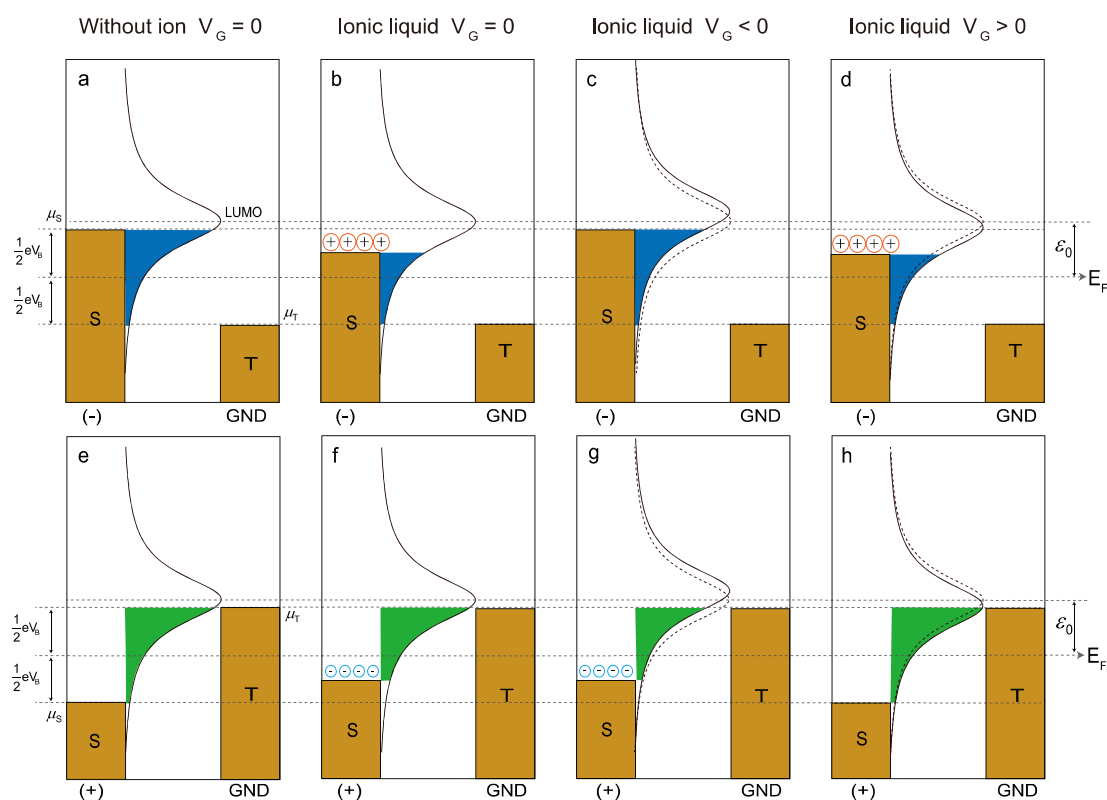


Figure 3. Illustrating the reversal of the rectifying direction in the molecular junction. Under zero bias, the molecular resonance with peak energy is ε_0 relative to the Fermi levels (E_F) of the substrate (S) and tip (T). The chemical potentials of the substrate and tip are denoted as μ_S and μ_T , respectively. (a,e) Schematic illustrating the energy level alignment in the molecular junction with (a) negatively and (e) positively biased substrates in the ion-absent environment. The chemical potentials of the substrate and tip shift symmetrically relative to the E_F of electrodes under negative bias and positive bias. The shaded area within the bias window of (a) is equal to the one of (e), indicating the absence of rectification. (b,f) Energy level alignment of the junction with (b) negatively and (f) positively biased substrates without gating voltage in the ionic liquid environment. The cations (anions) adsorb on the negatively (positively) biased electrode. (c,g) Energy alignment upon a negative gating voltage in ionic liquid. The negative gating voltage reduces the number of cations adsorbed on the substrate. Meanwhile, the negative gating voltage pushes the LUMO away from E_F . The dashed lines indicate the original transmission curves without a gating voltage. The area of (c) is larger than the one of (b), while the area of (g) is smaller than the one of (f), showing an opposite change trend under negative bias and positive bias. (d,h) Energy alignment of the junction upon a positive gating voltage. The number of anions adsorbed on the bottom substrate is modulated by the positive gating voltage. The area of (c) is larger than the one of (g) under negative gating voltage, while the area of (d) is smaller than the one of (h) under positive gating voltage, demonstrating the reversal of the rectification.

conductance–displacement traces. It shows that the probable conductance of the molecular junctions under a positive bias voltage ($V_B = 0.5$ V) is greater than that under a negative bias voltage ($V_B = -0.5$ V) when a positive gating voltage ($V_G = 0.3$ V) is applied. However, this situation is reversed, i.e., the conductance under positive bias becomes lower than that under negative bias when a negative gating voltage ($V_G = -0.5$ V) is applied, as shown in the bottom panel of Figure 1b. More conductance histograms can be found in Supplementary Figure S3, confirming the reliability of the observation.

Reversal of the Rectifying Direction by Ionic Liquid Gating. To verify that the direction of rectification can be reversed by the gating voltage, current–voltage (I – V) measurements were carried out within a bias window ($-1, 1$ V). Hundreds of I – V curves were recorded during the suspension period of the STM tip, and the traces containing distinct single molecule features that sustained the entire voltage ramp were selected based on the machine learning method; see Supplementary Figures S4 and S5 for details. The resulting I – V curves were overlaid and compiled into a two-dimensional histogram (I – V density map), as shown in Figure 2. Notably, the I – V curves exhibit a capacitance effect due to

the redistribution of ions; see Supplementary Figure S6. Here, we shift the I – V curves along the X -axis to make them cross the origin of the coordinates for clarity. More I – V density maps under an intermediate gating voltage can be found in Supplementary Figure S7. We can find that the shape of the I – V curves is strongly influenced by the negative gating voltages (Figure 2a–e) but relatively weakly modulated by the positive gating voltages (Figure 2e–h). Notably, the I – V curves show rectification behavior when the gating voltage is set to zero (Figure 2e). Specifically, the current under positive bias steadily decreases but the current under negative bias gradually increases when the gating voltage is changed from 1.2 to -1.2 V, resulting in a reversal of the rectifying direction of the current. This finding indicates that a prototype of a single molecular bidirectional thyristor can be fabricated via ionic gating; see Supplementary Figure S8 for details.

To explore the role of the ions, we measured the I – V curves of the molecular junction in another kind of ionic liquid, diethylmethyl(2-methoxyethyl)ammonium bis-(trifluoromethylsulfonyl)imide ([DEME]⁺[TFSI][−]). In contrast to [BMI]⁺[PF₆][−] with a planar structure, the cation and anion of [DEME]⁺ [TFSI][−] possess stereoscopic configura-

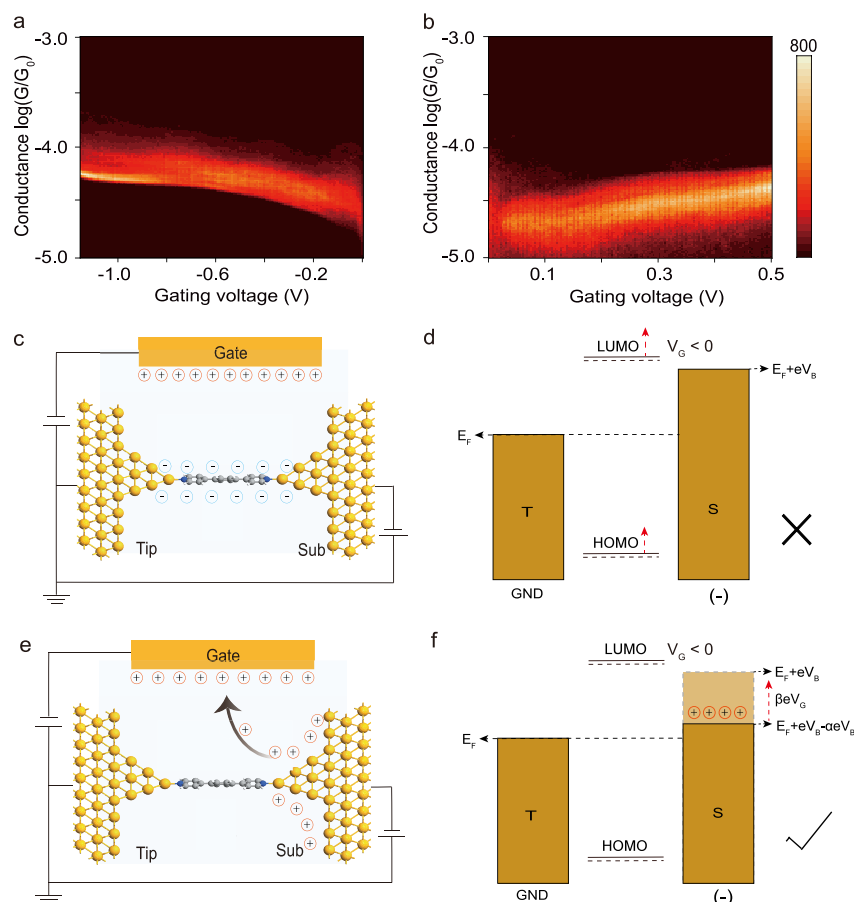


Figure 4. Conductance changes as a function of gating voltages and the analysis of the mechanisms. (a) Conductance of the junction increases as the gating voltage scans from 0 to -1.2 V under a fixed bias voltage (-0.1 V). (b) Conductance of the molecular junction increases as the gating voltage scans from 0 to -0.5 V at a fixed bias voltage (0.1 V). (c) Typical schematic of ion distribution upon a negative gating voltage. The anions accumulated around the molecular backbone due to the effect of negative gating voltage. (d) Typical mechanism of the molecular orbital gating upon a negative gating voltage. (e) Proposed ion distribution upon a negative gating voltage. The cations adsorbed on the substrate move toward the gating electrode as a negative voltage is applied to it. (f) Proposed mechanism for the ionic gating. The Fermi level of the substrate increases due to the reduced number of ions adsorbed on the substrate, resulting in the increase of current upon a negative gating voltage.

rations, leading to a less densely packed layer at the electrode interface.⁵⁵ The rectification feature for $[\text{DEME}]^+ [\text{TFSI}]^-$ is insignificant, and the reversal of rectification is not observed; see Supplementary Figures S9 and S10 for details. This control experiment indicates that the properties of ions themselves significantly influence the rectification characteristics.

Discussion of the Underlying Mechanisms. To understand the rectification behavior in the molecular junction, we considered a single-level transport model for current estimation, which is based on the Landauer formula by assuming a single-molecule orbital at energy ε_0 from the Fermi energy of the metal electrode (E_F), coupled via the coupling parameter Γ to the electrode.^{56–58} The current (I) can be expressed as

$$I = \frac{2e}{h} \int_{-eV/2}^{eV/2} T(E, \varepsilon, \Gamma) dE$$

Here, h is Planck's constant, e is the unit of charge, V is the applied voltage, and $T(E, \varepsilon, \Gamma)$ is the energy (E)-dependent transmission function. The current is proportional to the integral area under the transmission curve within the bias window ($-eV/2, eV/2$) when a bias (V) is applied.⁵²

Figure 3 shows the qualitative interpretation of the reversal of rectification from the energy alignment perspective. Despite

a clear asymmetry in $T(E, \varepsilon, \Gamma)$ with respect to the Fermi energy, Figure 3a,e shows identical integral areas (shaded in blue and green) that are independent of the bias polarity. The altering of the chemical potential of the electrode by changing its work function upon ion adsorption had been reported previously,⁵² which was further confirmed by the conductance measurements, see Supplementary Figure S11 for details. Figure 3b shows that the chemical potential of the negatively biased substrate (μ_s) decreases due to the adsorption of cations.⁵² Notably, the ion adsorption on the tip is not depicted in this figure considering that the tip is grounded, and thus, its chemical potential (μ_T) is less affected by the ion adsorption although the anions would adsorb on the tip due to the electric potential existing in the junction. By incorporating electrochemical impedance spectroscopy into the STM-BJ setup, the macroscopic characterization of ion adsorption can be directly demonstrated.⁵¹ Figure 3f shows that the chemical potential of the positively biased substrate increases because of the adsorption of anions. The integral area in Figure 3b is smaller than that in Figure 3f, which elucidates that the current under negative bias is smaller than that under positive bias, in line with the experimental rectification behavior, as shown in Figure 2e.

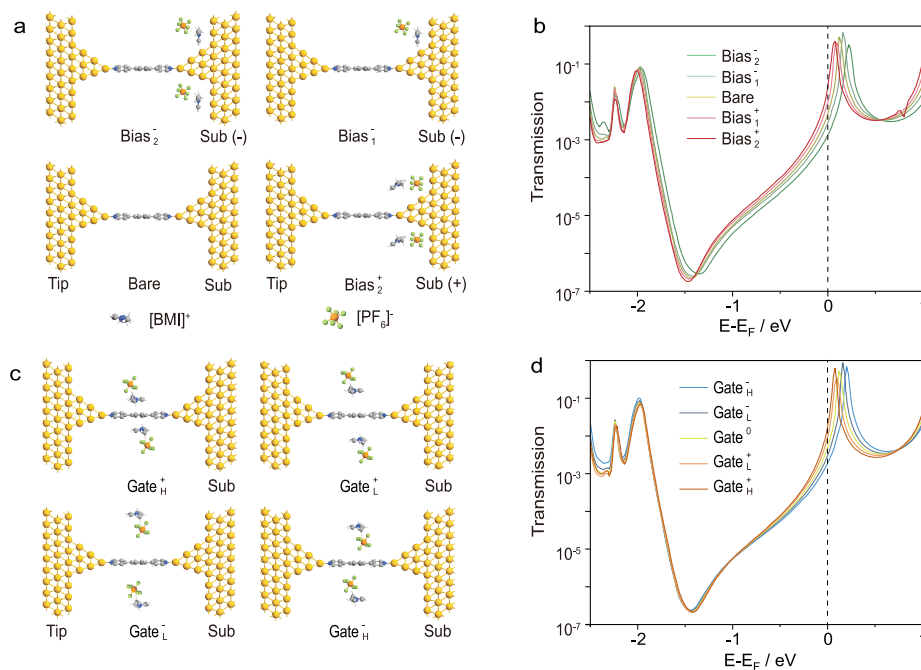


Figure 5. Calculation of transmission spectra of the molecular junction. (a) Schematic diagram of the BPB molecular junction under negative bias and positive bias without gating voltage. More anion–cation pairs are attracted to the substrate as the bias voltage increases. The [BMI]⁺ adsorbed closer on the substrate compared to [PF₆]⁻ when a negative bias voltage is applied. The alkyl chain substituent of [BMI]⁺ is simplified as methyl for clarity. (b) Calculated transmission functions of the molecular junction with the geometries presented in panel (a). LUMO moves closer to E_F when a negative bias is changed to a positive bias. (c) Schematic diagram of the BPB molecular junction upon gating voltage. Anion–cation pairs are accumulated around the molecule with [BMI]⁺([PF₆]⁻) located closer to the molecule upon a positive (negative) gating voltage. (d) Calculated transmission with the geometries presented in panel (c).

Figure 3c shows the energy landscape under a negative bias with a negative gating voltage. Compared with Figure 3b, the number of cations adsorbed on the substrate decreases upon a negative gating voltage (here, we reduced the number to zero for simplification). Meanwhile, the gating voltage electrostatically shifts the molecular orbitals relative to the Fermi level of electrode (E_F),²¹ i.e., the negative gating voltage pushes LUMO away from the E_F ,²³ see Supplementary Figure S12 for details. The integral area in Figure 3c is larger than that in Figure 3b, indicating that the current under a negative bias increases upon a negative gating voltage, consistent with the experimental observation presented in Figure 2a–d. Figure 3g shows the energy landscape of the junction under a positive bias upon a negative gating voltage. Here, the integral area of Figure 3c remains larger than that of Figure 3g, indicating that the current under negative bias exceeds that under positive bias, in line with the experimental observation shown in Figure 2a. Notably, if only part of the cations is removed from the substrate when the negative voltage is not large enough, the current under positive bias may equal to the one under negative bias; see Supplementary Figure S13 for details. This case fits with the experimental observation, in which symmetric I – V curves were observed under a gating voltage of -0.4 V.

Figure 3d,h shows the energy landscape under negative and positive biases upon a positive gating voltage, where the gating voltage pulls the LUMO closer to the E_F .¹⁰ The positive gating voltage greatly reduces the number of anions adsorbed on the substrate, as presented in Figure 3h. The area in Figure 3d is smaller than that in Figure 3c, while the area in Figure 3h is larger than that in Figure 3g, illustrating a reversal in the rectifying direction when the polarity of the gating voltage is changed. Also, we can find that the area of Figure 3d (Figure

3h) is similar to the area of Figure 3b (Figure 3f), indicating that the rectification direction is not changed when a positive gating voltage is applied, and the influence of positive gating voltage is relatively limited. In contrast, the area of Figure 3c (Figure 3g) changes a lot compared to the area of Figure 3b (Figure 3f), suggesting the significant effect of negative gating voltage, consistent with the experimental findings depicted in Figure 2. Additionally, the energy landscape of the molecular junction for [DEME]⁺ [TFSI]⁻ is presented in Supplementary Figure S14, which provides a comprehensive explanation for the absence of reversal of rectification in the ionic liquid environments with less compacted ions.

Notably, upon the gating voltage, the shift of the molecular orbital affects the current under negative bias and positive bias synchronously without significantly changing the rectification ratio.¹⁰ Therefore, the reversal of the rectifying direction signifies that the effect of gating voltage on the molecular orbital does not predominate the electron transport. The trivial effect of gating voltage on the molecular orbital in ionic liquid is supported by the measurements of conductance vs applied gate potential, which shows a continuous increase in current with decreasing (increasing) negative (positive) gating voltage, as shown in Figure 4a,b, respectively. If the anions accumulate around the molecular backbone upon a negative gating voltage (Figure 4c), the molecular conduction orbital will be strongly affected and the LUMO would upshift (Figure 4d). It would result in the decrease of current due to the increased energy barrier ($E_{LUMO} - E_F$) for electron transport. The decrease in current derived from Figure 4c,d conflicts with the experimental observation, as shown in Figure 4a. Additionally, such an orbital modification is independent of the bias polarity,¹⁰ and both the negative current and positive current

decrease simultaneously, making the reversal of rectification almost impossible. Therefore, we claim that the direct molecular orbital gating mechanism, verified in a solid molecular transistor, should not dominate the electron transport in the ionic gating environment.

Instead, we believe that the cations adsorbing on the electrode will migrate to the CE and RE due to the attraction force, as shown in Figure 4e. Notably, the voltage applied on the CE is larger than the voltage applied on the RE in our system, as mentioned previously, and the CE rather than the RE is put closer to the molecular junction. Therefore, the cations will mainly migrate to CE instead of RE. Due to the cation adsorption, the Fermi level of the biased substrate decreases from $E_F + eV_B$ to $E_F + eV_B - \alpha eV_B$, as shown in Figure 4f. When the adsorbed cations are removed from the substrate upon a negative gating voltage, the Fermi level of the substrate increases by βeV_G . Here, α and β denote the modulation efficiency of bias voltage and gating voltage on the chemical potential of the electrode. The increase of the Fermi level leads to an increase of the tunneling current, agreeing well with the experimental observation presented in Figure 4a. Therefore, we conclude that the modulation of the electrode's chemical potential rather than the regulation of molecular orbitals dominates the electron transport in the asymmetric ionic gating processes.

The stronger effect of gating voltage on EDL than the effect on the molecular orbital is reasonable. The ions adsorbed on the biased electrode moving toward the CE (RE) due to electrostatic attraction will directly reduce the number of ions adsorbed on the biased electrode and thus strongly affect the chemical potential of the electrode. In contrast, the ions move to the CE (RE) only indirectly promotes the accumulation of the ions around the molecule backbone by reducing the concentration of another kind of counterions in solution. Such accumulated ions are prone to diffusion in liquid due to the Coulomb repulsion, and thus the gating effect on the molecular orbital might be relatively trivial.

Theoretical Calculations. The change in the number of anion–cation pairs adsorbed on the electrode is used to model the change in the EDL, as shown in Figure 5a. Bias_\pm (Bias_\pm^+) represents one ion pair adsorbed on the negatively (positively) biased substrate with the cation (anion) located closer to the substrate surface. As the bias voltage increases, the number of ion pairs adsorbed on the electrode increases. The calculated transmission spectra, as shown in Figure 5b, demonstrate that the LUMO shifts to the right, moving away from E_F as more cations adsorb onto the substrate. The E_F of the electrode shifts downward with respect to the LUMO upon cation adsorption, confirming the previous claim that the chemical potential of the substrate (μ_s) decreases (downward shift) due to the adsorption of cations.

Additionally, we investigated how gating voltage impacts modulation of the electron transport through the molecular junction. A higher gating voltage brings the accumulated ion pair closer to the molecular backbone, as shown in Figure 5c. Here, Gate_\pm^- (Gate_\pm^-) denotes the situations in which a high (low) negative gating voltage is applied, causing the ion pairs to be located closer to (farther from) the backbone of BPB. Notably, the moiety of $[\text{BMI}]^+$ is located closer to the molecular backbone upon a positive gating voltage, while $[\text{PF}_6]^-$ is located closer to the molecule upon a negative gating voltage. The calculated transmission functions with different gating voltages are shown in Figure 5d. As the positive

(negative) gating voltage increases, the LUMO shifts closer (away) to the E_F of the electrode, which supports the claim made in Figure 3. Notably, this gating effect on molecular orbital is trivial compared to the effect on chemical potential of the electrode in the ionic liquid environment, which contrasts with the typical mechanism of solid molecular FET. Nevertheless, a positive superposition of the electrode's chemical potential gating effect and molecular orbital gating effect will greatly increase the gating efficiency, showing an advantage in the fabrication of multifunctional devices.

SUMMARY

We developed a technique to create single-molecule rectification using symmetric electrode materials and a molecular structure. More importantly, we demonstrated that the direction of current rectification can be fully reversed in situ by ionic liquid gating with densely packed ions on the electrode surface. This reveals that the effect of gating voltage on the chemical potential of the electrode in an asymmetric ionic liquid rather than the effect of gating voltage on the molecular orbital of the molecule dominates the electron transport, in contrast to the mechanism of solid molecule-based FET. Our work offers an approach for controlling electron transport through nanoscale objects and provides a principle for the fabrication of multifunctional devices, such as transistors, diodes, and thyristors, extending beyond single-molecule junctions.

METHODS

Four-Terminal STM-BJ. The STM-BJ configuration consists of a top gold tip encapsulated with Apiezon wax, which works as the drain electrode, and the bottom flat gold substrate serves as the source electrode. An Ag/AgCl electrode is introduced into the dynamic break junctions, serving as the RE, which significantly diminishes the influence of electrode polarization and solution voltage drop, resulting in precise control over the working electrode's potential. A platinum wire serves as the CE.

DFT-Based Calculation. To gain in-depth insights into the reversal of rectifying direction in single-molecule junctions, we conducted the transmission calculations under varied bias and gating voltage using density functional theory (DFT) combined with nonequilibrium Green's functions (NEGF); see Supplementary Figure S12 for detailed information. Additional calculations reveal that the distance between the ion pair and the electrode has minimal effect on the transmission function (Figure S15), highlighting the important role of ion density and thus changing intensity on the electrode surface.

ASSOCIATED CONTENT

Data Availability Statement

The data supporting the findings of this study are included in the published article and its Supporting Information or available from the corresponding authors on request.

Supporting Information

The Supporting Information is available free of charge at <https://pubs.acs.org/doi/10.1021/jacs.4c13773>.

Fabrication of the insulated tip electrode; asymmetric change of the electrostatic environment around the junction; conductance measurement by STM-BJ, I–V measurements, and voltage scanning process; processing method for I–V curves; effect of capacity in the ionic liquid environment; reversal of the rectifying direction; single molecular thyristor; origin of the rectification behavior; gating effect on I–V curves in two kinds of

ionic liquids; conductance of the molecular junction in ionic liquid and nonpolar TCB; gating voltage effect on the electron transport through the molecular junction; energy alignment of the molecular junction in [DEME]⁺[TFSI]⁻; and effect of distance between the ion pair and electrode on the electron transport (PDF)

AUTHOR INFORMATION

Corresponding Authors

Lichuan Chen – Institute of Modern Optics and Center of Single-Molecule Sciences, Tianjin Key Laboratory of Micro-scale Optical Information Science and Technology, Nankai University, Tianjin 300350, China; Email: chen_lichuan@126.com

Dong Xiang – Institute of Modern Optics and Center of Single-Molecule Sciences, Tianjin Key Laboratory of Micro-scale Optical Information Science and Technology, Nankai University, Tianjin 300350, China; orcid.org/0000-0002-5632-6355; Email: xiangdongde@nankai.edu.cn

Authors

Haoyu Wang – Institute of Modern Optics and Center of Single-Molecule Sciences, Tianjin Key Laboratory of Micro-scale Optical Information Science and Technology, Nankai University, Tianjin 300350, China

Fenglu Hu – Institute of Modern Optics and Center of Single-Molecule Sciences, Tianjin Key Laboratory of Micro-scale Optical Information Science and Technology, Nankai University, Tianjin 300350, China

Adila Adijiang – Institute of Modern Optics and Center of Single-Molecule Sciences, Tianjin Key Laboratory of Micro-scale Optical Information Science and Technology, Nankai University, Tianjin 300350, China

Ramya Emusani – Institute of Modern Optics and Center of Single-Molecule Sciences, Tianjin Key Laboratory of Micro-scale Optical Information Science and Technology, Nankai University, Tianjin 300350, China

Jieyi Zhang – Institute of Modern Optics and Center of Single-Molecule Sciences, Tianjin Key Laboratory of Micro-scale Optical Information Science and Technology, Nankai University, Tianjin 300350, China

Qihong Hu – Institute of Modern Optics and Center of Single-Molecule Sciences, Tianjin Key Laboratory of Micro-scale Optical Information Science and Technology, Nankai University, Tianjin 300350, China

Xuefeng Guo – Institute of Modern Optics and Center of Single-Molecule Sciences, Tianjin Key Laboratory of Micro-scale Optical Information Science and Technology, Nankai University, Tianjin 300350, China; Beijing National Laboratory for Molecular Sciences, National Biomedical Imaging Center, College of Chemistry and Molecular Engineering, Peking University, Beijing 100871, China; orcid.org/0000-0001-5723-8528

Takhee Lee – Department of Physics and Astronomy, and Institute of Applied Physics, Seoul National University, Seoul 08826, Korea; orcid.org/0000-0001-5988-5219

Complete contact information is available at:

<https://pubs.acs.org/10.1021/jacs.4c13773>

Notes

The authors declare no competing financial interest.

ACKNOWLEDGMENTS

This research was supported by the National Key R&D Program of China (no. 2021YFA1200103), the National Natural Science Foundation of China (nos. 22273041, 91950116, 12174201), the Natural Science Foundation of Tianjin (nos. 19JCZDJC31000, 19JCJQC60900, 22JCYBJC01310), and the China Postdoctoral Science Foundation (no. 2021M691871). The authors thank X-Tech for the STM-BJ.

REFERENCES

- (1) Su, T. A.; Neupane, M.; Steigerwald, M. L.; Venkataraman, L.; Nuckolls, C. Chemical principles of single-molecule electronics. *Nat. Rev. Mater.* **2016**, *1*, 16002.
- (2) Sun, L.; Diaz-Fernandez, Y. A.; Gschneidner, T. A.; Westerlund, F.; Lara-Avila, S.; Moth-Poulsen, K. Single-molecule electronics: from chemical design to functional devices. *Chem. Soc. Rev.* **2014**, *43*, 7378–7411.
- (3) Xiang, D.; Wang, X.; Jia, C.; Lee, T.; Guo, X. Molecular-scale electronics: from concept to function. *Chem. Rev.* **2016**, *116*, 4318–4440.
- (4) Tan, M.; Sun, F.; Zhao, X.; Zhao, Z.; Zhang, S.; Xu, X.; Adijiang, A.; Zhang, W.; Wang, H.; Wang, C.; Li, Z.; Scheer, E.; Xiang, D. Conductance evolution of photoisomeric single-molecule junctions under ultraviolet irradiation and mechanical stretching. *J. Am. Chem. Soc.* **2024**, *146*, 6856–6865.
- (5) Zhao, X.; Yan, Y.; Tan, M.; Zhang, S.; Xu, X.; Zhao, Z.; Wang, M.; Zhang, X.; Adijiang, A.; Li, Z.; Scheer, E.; Xiang, D. Molecular dimer junctions forming: Role of disulfide bonds and electrode-compression-time. *SmartMat* **2024**, *5*, No. e1280.
- (6) Zou, Q.; Qiu, J.; Zang, Y.; Tian, H.; Venkataraman, L. Modulating single-molecule charge transport through external stimulus. *eScience* **2023**, *3*, No. 100115.
- (7) Moth-Poulsen, K.; Bjørnholm, T. Molecular electronics with single molecules in solid-state devices. *Nat. Nanotechnol.* **2009**, *4*, 551–556.
- (8) Perrin, M. L.; Burzurí, E.; van der Zant, H. S. J. Single-molecule transistors. *Chem. Soc. Rev.* **2015**, *44*, 902–919.
- (9) Perrin, M. L.; Verzijl, C. J. O.; Martin, C. A.; Shaikh, A. J.; Eelkema, R.; van Esch, J. H.; van Ruitenbeek, J. M.; Thijssen, J. M.; van der Zant, H. S. J.; Dulić, D. Large tunable image-charge effects in single-molecule junctions. *Nat. Nanotechnol.* **2013**, *8*, 282–287.
- (10) Song, H.; Kim, Y.; Jang, Y. H.; Jeong, H.; Reed, M. A.; Lee, T. Observation of molecular orbital gating. *Nature* **2009**, *462*, 1039–1043.
- (11) Xiang, D.; Jeong, H.; Kim, D.; Lee, T.; Cheng, Y.; Wang, Q.; Mayer, D. Three-terminal single-molecule junctions formed by mechanically controllable break junctions with side gating. *Nano Lett.* **2013**, *13*, 2809–2813.
- (12) Xu, B.; Xiao, X.; Yang, X.; Zang, L.; Tao, N. Large gate modulation in the current of a room temperature single molecule transistor. *J. Am. Chem. Soc.* **2005**, *127*, 2386–2387.
- (13) Bai, J.; Li, X.; Zhu, Z.; Zheng, Y.; Hong, W. Single-molecule electrochemical transistors. *Adv. Mater.* **2021**, *33*, No. 2005883.
- (14) Huang, C.; Rudnev, A. V.; Hong, W.; Wandlowski, T. Break junction under electrochemical gating: testbed for single-molecule electronics. *Chem. Soc. Rev.* **2015**, *44*, 889–901.
- (15) Zhou, L.; Zhang, M.; Huo, Y.; Bai, L.; He, S.; Wang, J.; Jia, C.; Guo, X. Application of ionic liquids in single-molecule junctions: Recent advances and prospects. *Green. Energy Environ.* **2024**, *9*, 1784–1801.
- (16) Chen, S.; Frenzel, F.; Cui, B.; Gao, F.; Campanella, A.; Funtan, A.; Kremer, F.; Parkin, S. S. P.; Binder, W. H. Gating effects of conductive polymeric ionic liquids. *J. Mater. Chem. C* **2018**, *6*, 8242–8250.

- (17) Chen, F.; He, J.; Nuckolls, C.; Roberts, T.; Klare, J. E.; Lindsay, S. A. Molecular switch based on potential-induced changes of oxidation state. *Nano Lett.* **2005**, *5*, 503–506.
- (18) Kay, N. J.; Higgins, S. J.; Jeppesen, J. O.; Leary, E.; Lycoops, J.; Ulstrup, J.; Nichols, R. J. Single-molecule electrochemical gating in ionic liquids. *J. Am. Chem. Soc.* **2012**, *134*, 16817–16826.
- (19) Pobelov, I. V.; Li, Z.; Wandlowski, T. Electrolyte gating in redox-active tunneling junctions—an electrochemical STM approach. *J. Am. Chem. Soc.* **2008**, *130*, 16045–16054.
- (20) Tang, C.; Huang, L.; Sangtarash, S.; Noori, M.; Sadeghi, H.; Xia, H.; Hong, W. Reversible switching between destructive and constructive quantum interference using atomically precise chemical gating of single-molecule junctions. *J. Am. Chem. Soc.* **2021**, *143*, 9385–9392.
- (21) Capozzi, B.; Chen, Q.; Darancet, P.; Kotiuga, M.; Buzzeo, M.; Neaton, J. B.; Nuckolls, C.; Venkataraman, L. Tunable charge transport in single-molecule junctions via electrolytic gating. *Nano Lett.* **2014**, *14*, 1400–1404.
- (22) Wang, Z.; Palma, J. L.; Wang, H.; Liu, J.; Zhou, G.; Ajayakumar, M. R.; Feng, X.; Wang, W.; Ulstrup, J.; Kornyshev, A. A.; Li, Y.; Tao, N. Electrochemically controlled rectification in symmetric single-molecule junctions. *Proc. Natl. Acad. Sci. U. S. A.* **2022**, *119*, No. e2122183119.
- (23) Xin, N.; Li, X.; Jia, C.; Gong, Y.; Li, M.; Wang, S.; Zhang, G.; Yang, J.; Guo, X. Tuning charge transport in aromatic-ring single-molecule junctions via ionic-liquid gating. *Angew. Chem., Int. Ed.* **2018**, *57*, 14026–14031.
- (24) Li, Y.; Buerkle, M.; Li, G.; Rostamian, A.; Wang, H.; Wang, Z.; Bowler, D. R.; Miyazaki, T.; Xiang, L.; Asai, Y.; Zhou, G.; Tao, N. Gate controlling of quantum interference and direct observation of anti-resonances in single molecule charge transport. *Nat. Mater.* **2019**, *18*, 357–363.
- (25) Osorio, H. M.; Catarelli, S.; Cea, P.; Gluyas, J. B. G.; Hartl, F.; Higgins, S. J.; Leary, E.; Low, P. J.; Martín, S.; Nichols, R. J.; Tory, J.; Ulstrup, J.; Vezzoli, A.; Milan, D. C.; Zeng, Q. Electrochemical Single-Molecule Transistors with Optimized Gate Coupling. *J. Am. Chem. Soc.* **2015**, *137*, 14319–14328.
- (26) Metzger, R. M. Unimolecular electrical rectifiers. *Chem. Rev.* **2003**, *103*, 3803–3834.
- (27) Ni, L.; Li, X.; Zhao, Z.; Nam, J.; Wu, P.; Wang, Q.; Lee, T.; Liu, H.; Xiang, D. Reversible rectification of microscale ferroelectric junctions employing liquid metal electrodes. *ACS Appl. Mater. Interfaces* **2021**, *13*, 29885–29893.
- (28) Gupta, R.; Fereiro, J. A.; Bayat, A.; Pritam, A.; Zharnikov, M.; Mondal, P. C. Nanoscale molecular rectifiers. *Nat. Rev. Chem.* **2023**, *7*, 106–122.
- (29) Díez-Pérez, I.; Hihath, J.; Lee, Y.; Yu, L.; Adamska, L.; Kozhushner, M. A.; Oleynik, I. L.; Tao, N. Rectification and stability of a single molecular diode with controlled orientation. *Nat. Chem.* **2009**, *1*, 635–641.
- (30) Lörtscher, E.; Gotsmann, B.; Lee, Y.; Yu, L.; Rettner, C.; Riel, H. Transport properties of a single-molecule diode. *ACS Nano* **2012**, *6*, 4931–4939.
- (31) Yuan, L.; Nerngchamnong, N.; Cao, L.; Hamoudi, H.; del Barco, E.; Roemer, M.; Sriramula, R. K.; Thompson, D.; Nijhuis, C. A. Controlling the direction of rectification in a molecular diode. *Nat. Commun.* **2015**, *6*, 6324.
- (32) Atesci, H.; Kaliginedi, V.; Celis Gil, J. A.; Ozawa, H.; Thijssen, J. M.; Broekmann, P.; Haga, M.-A.; van der Molen, S. J. Humidity-controlled rectification switching in ruthenium-complex molecular junctions. *Nat. Nanotechnol.* **2018**, *13*, 117–121.
- (33) Souto, M.; Yuan, L.; Morales, D. C.; Jiang, L.; Ratera, I.; Nijhuis, C. A.; Veciana, J. Tuning the rectification ratio by changing the electronic nature (open-shell and closed-shell) in donor–acceptor self-assembled monolayers. *J. Am. Chem. Soc.* **2017**, *139*, 4262–4265.
- (34) Chen, X.; Roemer, M.; Yuan, L.; Du, W.; Thompson, D.; del Barco, E.; Nijhuis, C. A. Molecular diodes with rectification ratios exceeding 10^5 driven by electrostatic interactions. *Nat. Nanotechnol.* **2017**, *12*, 797–803.
- (35) Guo, C.; Wang, K.; Zerah-Harush, E.; Hamill, J.; Wang, B.; Dubi, Y.; Xu, B. Molecular rectifier composed of DNA with high rectification ratio enabled by intercalation. *Nat. Chem.* **2016**, *8*, 484–490.
- (36) Zhao, J.-M.; Chen, L.-Y.; Li, Y.-J.; Shi, N.-P.; Sun, Y.-Z.; Huang, H.; Zhang, G.-P. Greatly improving the rectifying performance of single-molecule diodes through molecular structure design and electrode material optimization. *Phys. E* **2021**, *130*, No. 114691.
- (37) Zhang, G.-P.; Chen, L.-Y.; Zhao, J.-M.; Sun, Y.-Z.; Shi, N.-P.; Wang, M.-L.; Hu, G.-C.; Wang, C.-K. Large Rectification Ratio of up to 106 for Conjugation-Group-Terminated Undecanethiolate Single-Molecule Diodes on Pt Electrodes. *J. Phys. Chem. C* **2021**, *125*, 20783–20790.
- (38) Wang, K.; Zhou, J.; Hamill, J. M.; Xu, B. Measurement and understanding of single-molecule break junction rectification caused by asymmetric contacts. *J. Chem. Phys.* **2014**, *141*, No. 054712.
- (39) Batra, A.; Darancet, P.; Chen, Q.; Meisner, J. S.; Widawsky, J. R.; Neaton, J. B.; Nuckolls, C.; Venkataraman, L. Tuning rectification in single-molecular diodes. *Nano Lett.* **2013**, *13*, 6233–6237.
- (40) Kim, T.; Liu, Z.-F.; Lee, C.; Neaton, J. B.; Venkataraman, L. Charge transport and rectification in molecular junctions formed with carbon-based electrodes. *Proc. Natl. Acad. Sci. U.S.A.* **2014**, *111*, 10928–10932.
- (41) Kornyshev, A. A.; Kuznetsov, A. M.; Ulstrup, J. In situ superexchange electron transfer through a single molecule: A rectifying effect. *Proc. Natl. Acad. Sci. U.S.A.* **2006**, *103*, 6799–6804.
- (42) Nerngchamnong, N.; Yuan, L.; Qi, D.-C.; Li, J.; Thompson, D.; Nijhuis, C. A. The role of van der Waals forces in the performance of molecular diodes. *Nat. Nanotechnol.* **2013**, *8*, 113–118.
- (43) Yamada, R.; Albrecht, K.; Ohto, T.; Minode, K.; Yamamoto, K.; Tada, H. Single-molecule rectifiers based on voltage-dependent deformation of molecular orbitals in carbazole oligomers. *Nanoscale* **2018**, *10*, 19818–19824.
- (44) Baghbanzadeh, M.; Belding, L.; Yuan, L.; Park, J.; Al-Sayah, M. H.; Bowers, C. M.; Whitesides, G. M. Dipole-induced rectification across AgTS/SAM//Ga₂O₃/EGaIn junctions. *J. Am. Chem. Soc.* **2019**, *141*, 8969–8980.
- (45) Perrin, M. L.; Galán, E.; Eelkema, R.; Thijssen, J. M.; Grozema, F.; van der Zant, H. S. J. A gate-tunable single-molecule diode. *Nanoscale* **2016**, *8*, 8919–8923.
- (46) Zhang, N.; Lo, W.-Y.; Cai, Z.; Li, L.; Yu, L. Molecular rectification tuned by through-space gating effect. *Nano Lett.* **2017**, *17*, 308–312.
- (47) Sawano, F.; Terasaki, I.; Mori, H.; Mori, T.; Watanabe, M.; Ikeda, N.; Nogami, Y.; Noda, Y. An organic thyristor. *Nature* **2005**, *437*, 522–524.
- (48) Bai, J.; Daaoub, A.; Sangtarash, S.; Li, X.; Tang, Y.; Zou, Q.; Sadeghi, H.; Liu, S.; Huang, X.; Tan, Z.; Liu, J.; Yang, Y.; Shi, J.; Mészáros, G.; Chen, W.; Lambert, C.; Hong, W. Anti-resonance features of destructive quantum interference in single-molecule thiophene junctions achieved by electrochemical gating. *Nat. Mater.* **2019**, *18*, 364–369.
- (49) Xu, B.; Tao, N. J. Measurement of Single-Molecule Resistance by Repeated Formation of Molecular Junctions. *Science* **2003**, *301*, 1221–1223.
- (50) Kotiuga, M.; Darancet, P.; Arroyo, C. R.; Venkataraman, L.; Neaton, J. B. Adsorption-induced solvent-based electrostatic gating of charge transport through molecular junctions. *Nano Lett.* **2015**, *15*, 4498–4503.
- (51) Shi, W.; Greenwald, J. E.; Venkataraman, L. Impact of solvent electrostatic environment on molecular junctions probed via electrochemical impedance spectroscopy. *Nano Lett.* **2024**, *24*, 9283–9288.
- (52) Capozzi, B.; Xia, J.; Adak, O.; Dell, E. J.; Liu, Z.-F.; Taylor, J. C.; Neaton, J. B.; Campos, L. M.; Venkataraman, L. Single-molecule diodes with high rectification ratios through environmental control. *Nat. Nanotechnol.* **2015**, *10*, 522–527.
- (53) Zhang, W.; Zhao, Z.; Tan, M.; Adijiang, A.; Zhong, S.; Xu, X.; Zhao, T.; Ramya, E.; Sun, L.; Zhao, X.; Fan, Z.; Xiang, D. Regulating the orientation of a single coordinate bond by the synergistic action of

mechanical forces and electric field. *Chem. Sci.* **2023**, *14*, 11456–11465.

(54) Jin, W.; Liu, X.; Han, Y.; Li, S.; Yan, T. Effects of repulsive interaction on the electric double layer of an imidazolium-based ionic liquid by molecular dynamics simulation. *Phys. Chem. Chem. Phys.* **2015**, *17*, 2628–2633.

(55) Kim, Y.-J.; Matsuzawa, Y.; Ozaki, S.; Park, K. C.; Kim, C.; Endo, M.; Yoshida, H.; Masuda, G.; Sato, T.; Dresselhaus, M. S. High energy-density capacitor based on ammonium salt type ionic liquids and their mixing effect by propylene carbonate. *J. Electrochem. Soc.* **2005**, *152*, A710.

(56) Huisman, E. H.; Guédon, C. M.; van Wees, B. J.; van der Molen, S. J. Interpretation of transition voltage spectroscopy. *Nano Lett.* **2009**, *9*, 3909–3913.

(57) Kim, Y.; Hellmuth, T. J.; Sysoiev, D.; Pauly, F.; Pietsch, T.; Wolf, J.; Erbe, A.; Huhn, T.; Groth, U.; Steiner, U. E.; Scheer, E. Charge transport characteristics of diarylethene photoswitching single-molecule junctions. *Nano Lett.* **2012**, *12*, 3736–3742.

(58) Taherinia, D.; Frisbie, C. D. Deciphering I–V characteristics in molecular electronics with the benefit of an analytical model. *Phys. Chem. Chem. Phys.* **2023**, *25*, 32305–32316.